fortune Journals

Research Article

FORTUNE JOURNAL OF RHEUMATOLOGY

ISSN: 2688-6766

Numerical Simulation of Pressure Distribution for Structural Design of Diabetic Footwear Insoles

Matthew Sin-hang Leung[1,2], Kit-lun Yick[1,2*], Yue Sun[3] and Sun-pui Ng[4]

Abstract

Diabetic foot ulcerations or open wounds that cannot heal on the feet are a serious condition for people who have diabetic mellitus, as they might face lower limb amputation if the wounds are not well cared. Here, we propose braced frame structure insoles with traditional insole material to further reduce the shear stress and contact pressure at the plantar-insole surface to reduce the risk of foot injury. Finite element models (FEMs) are developed to evaluate the structural changes of the developed braced frame structure upon exertion of compressive forces. Also, the effect of different braced frame structures on the shear stress, contact area as well as maximum contact force of the plantar are analysed through a finite element analysis (FEA). The result of the validated FEMs show that the proposed structure reduces the shear stress (~21%) and maximum contact force (~55%) more than traditional diabetic insoles.

Keywords: Diabetic; Foot ulcerations; Orthotic footwear insoles; Diabetic mellitus.

Introduction

Diabetic mellitus is a major health epidemic around the world. One of the most detrimental and costly complications that diabetic patients experience are diabetic foot ulcers which frequently put diabetics at a high risk of lower limb amputation with a lifetime incidence of about 15-25% [1]. Diabetic foot ulcers impair the quality of life and affect social activities and livelihood. To reduce high plantar pressure, custom-fabricated orthotic footwear insoles are prescribed to redistribute the pressure in the different plantar regions. With the increasing prevalence of diabetes, orthotic insoles have become one of the most important means of preventing and managing excessive plantar pressure and diabetic foot ulcerations [2]. The materials used for insole fabrication are generally light in weight, pliable with a low Young's modulus and high energy absorption performance in order to absorb and distribute the impact forces during walking and daily activities. Traditional insole materials include polyurethane (PU) foam, leather and polyethylene (PE) foam of different qualities, densities and thicknesses are frequently used [3]. Insoles may also be prescribed in a 3D conforming shape to the feet to increase the contact surface between the plantar and the insole [4]. Unfortunately, due to the high variability of the foot shape, footwear needs and practical use amongst patients, the treatment outcome of orthotic insoles is somewhat unsatisfactory. Insole material structures and parameters such as stress-strain behaviour and shear force are not fully studied. Studies in the literature on insole shear stress between the plantar-insole interface have indicated that shear stresses on the diabetic foot not only show a close correlation with thermal changes

Affiliation:

[1]School of Fashion and Textiles, The Hong Kong Polytechnic University, Hung Hom, Kowloon, Hong Kong, China

[2]Laboratory for Artificial Intelligence in Design, Hong Kong Science Park, New Territories, Hong Kong, China

[3]School of Fashion Design & Engineering, Zhejiang Sci-Tech University, Hangzhou City, Zhejiang Province, China

[4]School of Professional Education and Executive Development, The Hong Kong Polytechnic University, Hung Hom, Kowloon, Hong Kong, China

***Corresponding author:**
Kit-lun Yick, 1School of Fashion and Textiles, The Hong Kong Polytechnic University, Hung Hom, Kowloon, Hong Kong, China

Laboratory for Artificial Intelligence in Design, Hong Kong Science Park, New Territories, Hong Kong, China

Citation: Matthew Sin-hang Leung, Kit-lun Yick, Yue Sun and Sun-pui Ng. Numerical Simulation of Pressure Distribution for Structural Design of Diabetic Footwear Insoles. Fortune Journal of Rheumatology. 6 (2024): 38-45.

Received: July 31, 2024
Accepted: August 08, 2024
Published: August 29, 2024

Leung MS., et al., Fortune J Rheumatol 2024
DOI:10.26502/fjr.26880042

in response to walking [5, 6], but also contribute up to 30% of the vertical loading on the foot [7]. Analysis of the material parameters is therefore important to better obtain insole materials that precisely control and manage the plantar pressure for optimal foot protection. While very little work has focused on internal structure of the insole materials [8, 9], new types of insole materials in a braced frame structure and their offloading behaviour are investigated in this study.

Braced frame structures are traditionally used to prevent excessive lateral loading by using diagonal steel members or shear cores in building construction. The structural system can resist wind and earthquake forces in the construction of buildings [10]. Normally, the members in a braced frame cannot be moved in the lateral direction. Beams and columns in the braced frame are rated under vertical loads, which assume that the bracing system contributes to all the loads in the lateral direction [11]. There are a wide range of braced framed structures, such as V-braced, X-braced and multi-storey-X-braced. The V-braced frame structure was designed to protect buildings from maximum unbalanced vertical and horizonal loads when there is buckling and yielding of the beam. However, the beams of a V-braced structure have to be very strong to maintain stability. While the X-braced structure and the multi-storey-X-braced structures have a low peak inter-storey drift ratio, they can balance the forces on the beams when there is buckling and yielding. In considering the reduced shear force energy with improved stability of braced frame structures [12], the potential use of X-braced and multi-storey-X-braced structures for insole material is investigated in this study. These two structures have a very low peak inter-storey drift ratio in all different braced framed structures, which means that they are more stable than the V-braced structure [13].

The density of insole materials is greatly associated with the energy absorption performance of insoles during wearing. When shear force is applied to the insole, the shear deformation reduces the volume of the insole which is calculated by using:

$$\rho = \frac{m}{V} \quad \ldots (1)$$

Where ρ is the density, m is the mass and V is the volume. The use of a braced framed structure may reduce the shear deformation of insole material [14], while the density of the insole can remain constant for minimal contact pressure between the plantar and the insole [15].

In order to obtain better control over pressure and reduce unavoidable errors from human wear trial such as the inconsistencies, a finite element model (FEM) is used to simulate pressure distribution on the insole. This is a very popular computational simulation method that is used to solve numerical problems that arise in engineering and mathematical modelling processes and enhance the understanding of biomechanical applications [16]. Hence, the use of an FEM in biomechanical research has been very common and successful due to the efficiency of modeling structures with asymmetric geometries and complex material properties [17, 18]. It is also possible to constantly modify simulations based on the changes in conditions or material factors like the dimensions and material properties, without the need to manufacture footwear or replicate subject trials. For example, Shaulian et al. [19] studied the foot by using FEM to simulate the location of heel strike when varying the depth of the unloaded hole below the foot ulcer on the insole. The study found that a large unloading radius, large radius of curvature, and large hole depth minimize pressure and therefore the risk of diabetic ulcers. Cheung et al. [20] developed an FEM of the foot including the bony structure, soft tissues, cartilage, ligaments and fascia to compare the pressure distribution by adding on a insole with a human wear trial. The model offers an efficient approach to assess the effects of different insole parameters and material properties on the reduction of peak plantar pressure. The FEM is an ideal clinical tool to understand the foot behaviour in different situations and explore the design of different forms of footwear.

In this study, we propose a new type of insole structure to reduce the maximum plantar pressure of diabetic patients. A FEM of the foot with bone models is constructed and slowly compressed onto the insole under half bearing of body weight to simulate a standing posture. A finite element analysis (FEA) is used to simulate the influence of the internal structure of the proposed insole on the redistribution of plantar pressure and the results are compared with those of a traditional insole structure with material of PE and PU foams.

Methodology

Design of braced frame structures and construction of insole sub-model

A total of three different braced frame structures are used as the internal structure of the insole material, including a square structure (SQ), a X-braced frame structure (XBF) and a Multi-storey-X-braced frame structure (MXBF) respectively. Their corresponding geometry and dimensions of the unit cell are shown in Figure 1. They are prepared with dimensions of 120 mm in width, 300 mm in length and 36 mm in height for insole applications [2]. The dimensions of the unit cells and the insole are kept constant, while the volume of the insoles varies with different internal structure designs (Table 1). Their mechanical properties and the pressure reduction performance are also compared with two traditional insole materials, including a PU foam (Poron®) and a PE foam (PeLite®).

Leung MS., et al., Fortune J Rheumatol 2024
DOI:10.26502/fjr.26880042

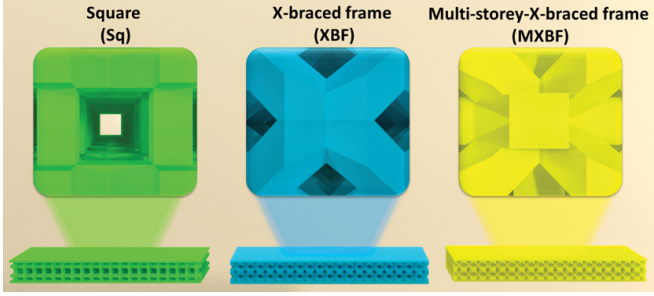

Figure 1: Internal structures of insole in a square (Sq), a X-braced frame (XBF) and a Multi-storey-X-braced frame (MXBF) structures.

Table 1: Volume of the insole with different internal structures

Insole Structure	Volume (mm^3)
Square (Sq)	4,96,000.00
X-braced frame (XBF)	7,55,133.72
Multi-storey-X-braced frame (MXBF)	8,97,045.70
Original (as control)	12,96,000.00

Mechanical characterization of the insole material

The compression properties of two traditional types of insole materials, PU foam (Poron®) and PE foam (PeLite®), were first measured. The ASTM D575 Standard Test Method for rubber properties in compression was referenced and the Instron 4411 universal mechanical test frame was used. The specimens are 28.5 mm in diameter and 12.5 mm in thickness. The results were then inputted into the FEM to simulate the interface pressure distribution during insole compression.

Three-dimensional scanning and modelling of foot sub-model

A structured light handheld 3D scanner (Artec Eva, Luxembourg) was used to obtain the geometry and shape of a non-weighted foot of a healthy male subject. The complex geometry and shape of the foot can be scanned accurately with this scanner. The scanned data were generated by using Artec Studio 13 and transformed into a 3D model. After obtaining the 3D model of the foot, the sub-model of the foot bones including distal phalange, metatarsal, cuboid, talus, calcaneus and tibia, as well as the designed insole and the foot were constructed into a mesh model by using MSC Apex software. After the mesh model was obtained, it was then constructed into an FEM by using FEA software (MSC Marc 2019.2.0, US) (Figures 2A and 2B). The material properties of the foot and bones were obtained with reference to Gefen et al. [21] (Table 2). The Young's modulus and Poisson's ratio for the bones and soft tissues are 7300 MPa and 0.3, 0.3MPa and 0.4 respectively. The element type of the insole is a structural 3-D solid element type 127, the foot and the bones are structural 3-D solid element type 134 [22], while the insole material is regarded as an Ogden elastomer model [23]. The following equation is used to determine the strain energy:

$$W_{deviatoric}^{ogden} = \sum_{k=1}^{N} \frac{\mu_k}{\alpha_k}\left(\bar{\lambda}_1^{\alpha_k} + \bar{\lambda}_2^{\alpha_k} + \bar{\lambda}_3^{\alpha_k} - 3\right) \quad \ldots(2)$$

where $\bar{\lambda}_1^{\alpha_k} = J^{-\frac{\alpha_k}{3}}\lambda_i^{\alpha_k}$ is the deviatoric stretch ratio while μ_k and α_k are the moduli and exponent constants obtained from the curve fitting of the experimental data. To validate the accuracy of the FE contact model, a compression test was done so that the simulated result was compared with the experimental compression result based on the ASTM D575 standard test method.

Table 2: Material properties and element type of the finite element model

Component	Element type	Young's modulus E (MPa)	Poisson's ratio v
Bones	3D-tetrahedra	7300	0.3
Soft tissues	3D-tetrahedra	0.3	0.4

To evaluate the plantar pressure in the standing position, an external force of 350 N (half weight of the subject) was applied onto the insole (see Figure 2C). To ensure all the force can be evenly applied onto the insole, a rigid link (RBE2) was set where each node on the bottom surface of the insole was rigidly connected to a corresponding node that was set under the insole, while the degree of freedom in all directions was also fixed. The nodes above the ankle of the foot were fixed in all directions and the bones inside the foot were set as a rigid body. The friction force tolerance was set to be 0.22 [24]. The shear stress, maximum contact force and total contact area of the plantar under the different structures of insole material were systematically investigated and compared.

Figure 2: FE foot models including (A) bones and (B) soft tissues so that (C) the boundary condition added to the insole sub-model can be simulated and optimised through an FEA

Result and Discussion

Compression properties

In order to withstand the deformation loads and retain the original shape of the insole material to reduce the plantar pressure, the compressive stress of the insole material is an important parameter. The stress-strain behaviour is one of the criteria to determine the performance of the insole. With a low Young's modulus, the insole can be easily deformed to absorb energy. The stress-strain cycle of traditional insole material is plotted in Figure 3 and the Young's modulus and

Leung MS., et al., Fortune J Rheumatol 2024
DOI:10.26502/fjr.26880042

Poisson's ratio values are listed in Table 3. The PE foam has a higher Young's modulus than that of the PU foam. PE foam tends to have better shape retention with less deformation as compared to the PU foam. The Young's modulus and Poisson's ratio values are applied to the FEM.

Table 3: Material properties of the insole material

Material	Young's modulus E (MPa)	Poisson's ratio v
PU foam (Poron®)	1	0.35
PE foam (PeLite®)	3	0.34

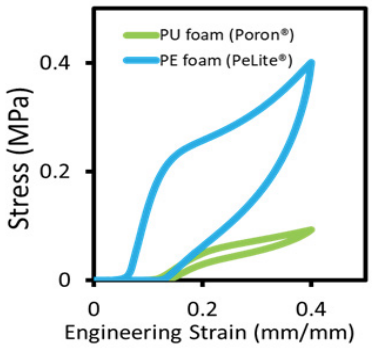

Figure 3: Plotted compression properties of insole material: stress-strain of PU foam vs PE foam

Validation of material properties through computational simulation

First, the reliability of the FEM is validated to confirm its ability to accurately predict the material compression behaviour by using a FEA. A compression test was carried out and the simulation results were compared with the experimentally obtained compression displacement values. The solid specimens for the FEM are 28.5 mm in diameter and 12.5 mm in thickness. A compression force of 350 N was applied to the specimens to measure their displacements. The results showed that the FEM can accurately predict the compression displacements of the PU and PE foams. As shown in Figure 4, the compression displacement results obtained from the simulation model is slightly higher than those from the experiments, but with less than a 3% discrepancy, while the friction during the experiment is negligible in the FEM.

Effect of insole internal structures on the insole-plantar interface

The FEM was then used to predict the influence of the proposed internal structure of the PU and PE foams on the plantar of the foot. The shear stress, contact area, as well as contact forces between the insole and plantar interface were then systematically analysed.

Shear stress: A 3D geometric sub-model of the human foot was developed to predict the shear stress of the soft tissues of the foot, the interface pressure between the foot and

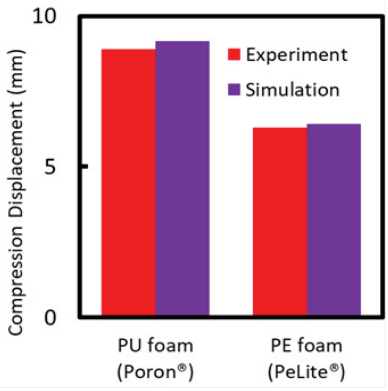

Figure 4: Validation of the developed FEM - Comparison of experiment and simulation results for PU and PE foams.

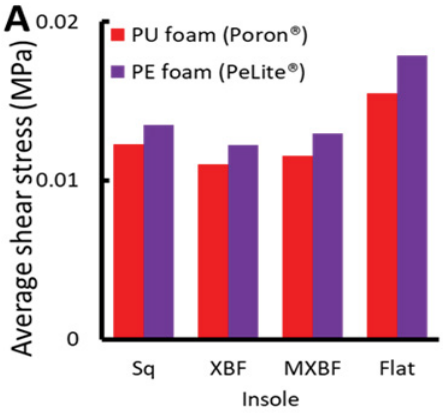

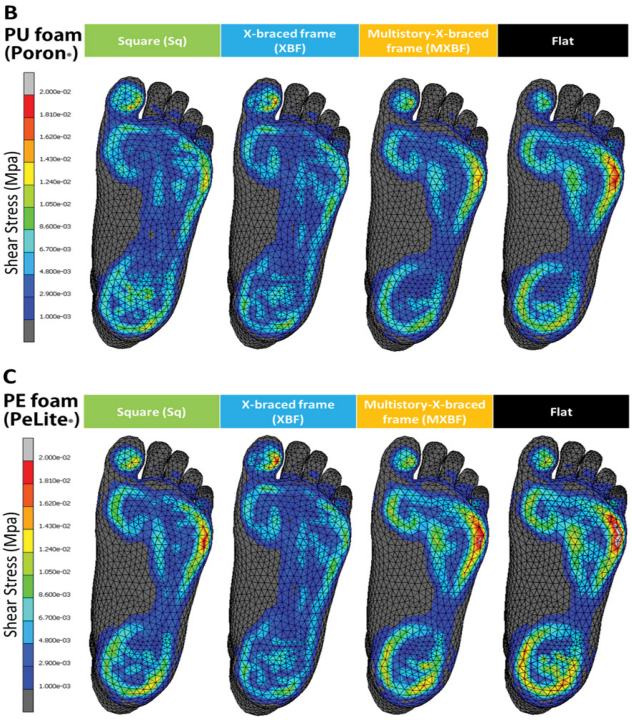

Figure 5: (A) Shear stress of PU and PE insoles with different internal structures; (B) Shear stress distribution of the plantar with various PU insole structures; and (C) PE insole structures.

Leung MS., et al., Fortune J Rheumatol 2024
DOI:10.26502/fjr.26880042

insole and the contact conditions during standing, when the different insoles are worn. The mean shear stress between the foot and the insole is shown in Figure 5A. The results indicate that the PU foam insoles show a lower shear force compared to the PE foam insoles by an average of 12%, which may be associated with the deformation behaviour of PE insoles. In both foams, the proposed braced frame structure results in a major reduction of the shear stress (21% or higher). As compared to the MXBF structure, the results show that the XBF structure has a lower shear stress. The shear stress reduction performance of the non-braced frame structure (Sq) is less effective, as compared to the braced frame structures (XBF and MXBF). The shear stress distribution between the foot and the insole for the various insole conditions is also obtained through simulation. As shown in Figures 5B and 5C, high shear stresses are found along the edge of the heel, metatarsals and the great toe, where the plantar soft tissues deform the most, thus leading to a high risk of foot pain and injury. The peak shear stress on the edge of the PU foam insole is lower than that of the PE foam insole (17% and higher). The braced frame structure has a low peak shear stress as compared to the non-braced frame structure (Sq). Therefore, the braced frame structure can reduce the peak and the mean shear stress of the plantar of the foot, which can greatly reduce the risk of becoming injured from shearing forces.

Contact area: Apart from the shear stress, insole designs with increased contact area between the insole and the plantar are primarily adopted to redistribute the plantar pressure, particularly during body movement for optimal foot protection from excessive plantar pressure and even ulcerations for diabetic patients. The contact area is determined by:

$$P = \frac{F}{A} \qquad \ldots(3)$$

where P is the pressure, F is the magnitude of the normal forces and A is the area of the surface on contact. As shown in Figure 6A, XBF shows a very high contact area in both the PU and PE foams while Sq and MXBF show a similar result in the total contact area. The original structure of the PU and PE insoles provides the smallest total contact area. As compared to the control, the braced frame structure of XBF tends to increase the contact area by 64% in the PU insole and 90% in the PE insole, at a load of 350 N. Therefore, XBF increases the contact area more effectively than non-braced frame structure (Sq) in both the PU (20%) and PE insoles (46%) (see Figure 6B). The percentage changes in volume between XBF and the non-braced frame structure (Sq)were then compared. The results showed that the volume of XBF is 52% larger than that of Sq. The changes in the internal structure between the two insoles are shown in Figure 6C. Under a compression load of 350 N, the space in the beam of the XBF insole is substantially reduced as compared to

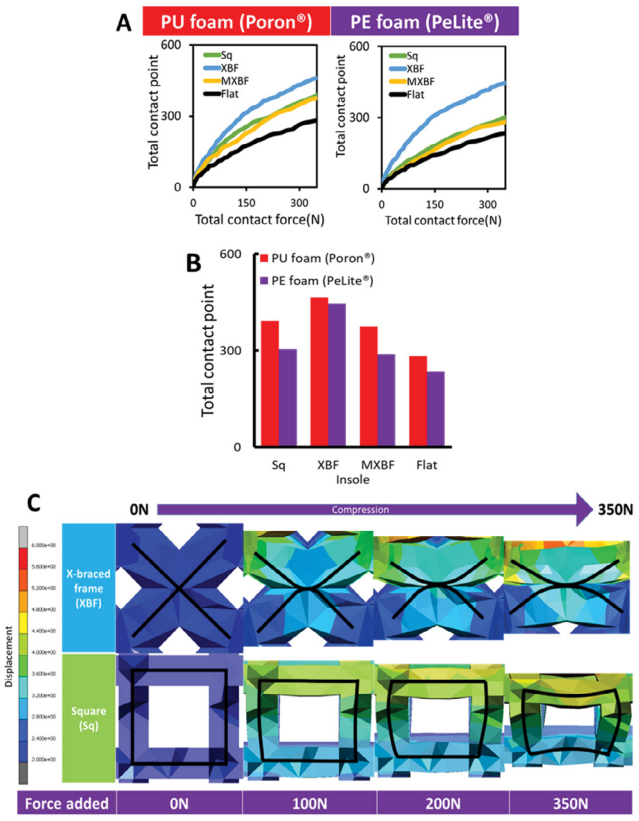

Figure 6: (A) Comparison of contact area of PU foam and PE foam with different internal structure. (B) Difference in contact area of PU foam and PE foam with different internal structure under load of 350 N. (C) Illustration of FEM in this study to predict changes with XBF and Sq insoles.

the Sq. The XBF insole structure can readily accommodate the curved interface of the plantar of the foot, hence leading to an increased contact area with the plantar. A simple FE simulation was carried out to obtain the compression behaviour of the insole structures. A compression force was applied onto a PU foam cuboid (length: 5 mm, width: 5 mm, and height: 10 mm) along two different directions (see Figure 7A). To compress a cuboid of 1 mm, a total force of 3.47 N is required while to bend a cuboid of 1 mm, the total force required is only 0.22 N. Apart from the FE, a mathematical analysis was done to compare the forces for compression and bending. The equation for compression stress is:

$$\sigma = \frac{\Delta L}{L_o} \mathrm{E} \qquad \ldots(4)$$

where σ is the compression stress, ΔL is the change in the length, L_o is the original length and E is the Young's modulus of the material. It was found that a force of 2.5 N is needed to compress 1 mm of cuboid. The equation for the bending stress is:

$$\sigma = \frac{Mc}{I} \qquad \ldots(5)$$

Leung MS., et al., Fortune J Rheumatol 2024
DOI:10.26502/fjr.26880042

$$I = \int_{Q} r^2 dm \quad \ldots(6)$$

where σ is the bending stress, M is the bending moment with respect to the centroidal axis, c is the radius of the centroidal axis, I is the bending moment of inertia, r is the distance to some potential rotation axis, and the integral is over all the infinitesimal elements of mass, dm, in a three-dimensional space occupied by object Q. The bending moment of the cuboid is $\frac{1}{3}ML^2$. Therefore, the force required to bend 1 mm of cuboid is 0.16 N. Both the FE and mathematical results show that 1500% less force is needed to bend than compress 1 mm of cuboid (see Figure 7B). Therefore, the XBF insole can be readily deformed with increase in contact area between the plantar and the insole.

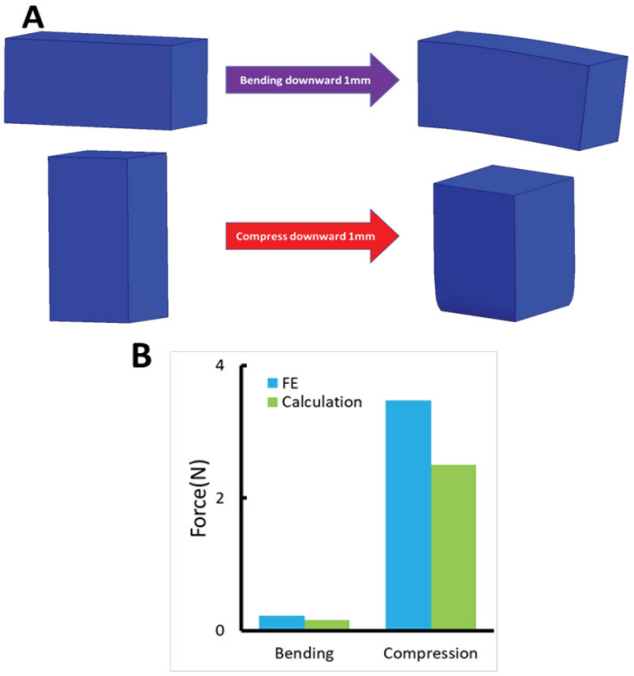

Figure 7: (A) Illustration of FEM changes with bending and compression. (B) Comparison of force - bending vs compression.

Contact pressure: The braced frame structure has a lower maximum contact force than that of the control condition; see Figure 8A. The maximum contact force of the XBF structure is 55% lower with the PU foam and 86% with the PE foam. Due to the smaller contact area of the non-braced frame structure (Sq), the maximum contact force is 4% higher in the PU foam and 8% higher in PE foam in comparison with XBF. The influence of the internal structure on the trajectory of the maximum contact force is negligible with both the PU and PE foams; see Figure 8B. It has been found that pressure is directly proportional to the applied force, but inversely proportional to the contact area. A material with a low Young's modulus tends to reduce the maximum contact force. In this study, PE foam with an XBF structure has a lower maximum contact force (54% or less) than the PU foam with a non-braced frame structure - (Sq and the control. The effect of the internal structure on material deformation is more apparent than the Young's modulus, which leads to the reduction of the insole-foot contact pressure. By looking at Figures 8C and 8D, a large amount of contact force is found at the heel and the metatarsals. The trend of the contact force pattern is similar to the distribution of the shear stress in the heel and the metatarsals which may result in potential foot pain and injury. As compared to the control insole, the proposed braced frame structure enables a better force distribution throughout the plantar with lower maximum contact forces.

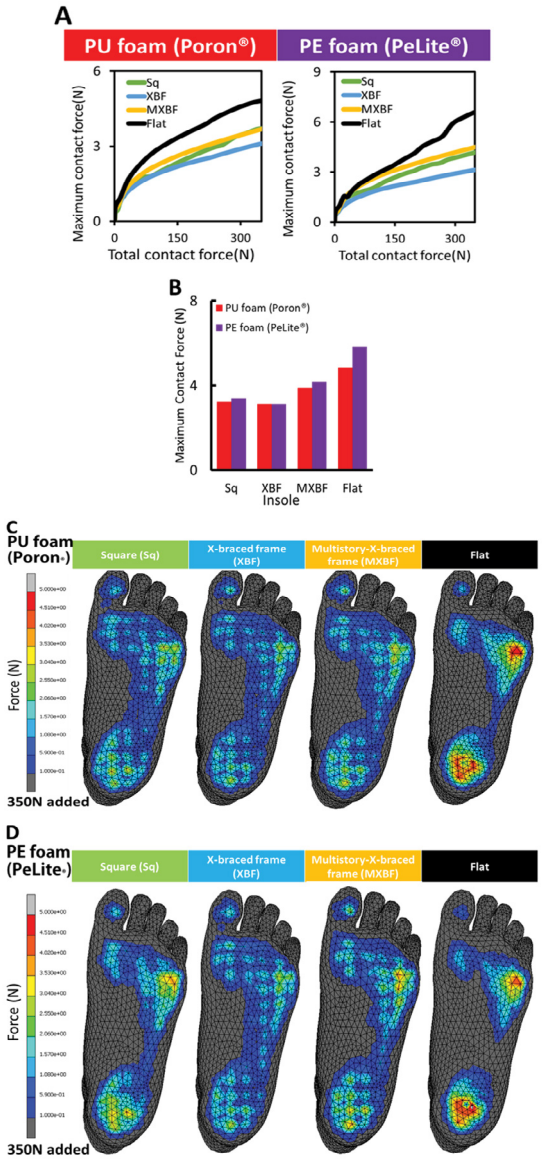

Figure 8: (A) Comparison of maximum contact force of PU foam and PE foam with different internal structures. (B) Difference in maximum contact forces of PU foam and PE foam with different internal structures under load of 350 N. (C and D) Contact force distribution of plantar using PU and PE foam insoles respectively.

Conclusion

Diabetic insoles are one of the most frequently used devices to protect the plantar of the foot from injury. However, the protection performance and outcomes of orthotic insoles are somewhat controversial. In this study, two novel braced frame structures are proposed to reduce the shear stress and the pressure interface between the insole and the plantar. An FEA is used to systematically determine the influence of the braced frame structures on shear stress, contact area and maximum contact force of the insole. A load of 350 N to simulate a standing posture is applied to the foot model. The results show that XBF can effectively reduce the shear stress and the maximum contact force, as compared to the control. The X-shape beams of the XBF structure can be readily compressed, thus conforming to the curvature of the foot with increased contact area. The findings of this study provide useful information and insights to manufacturers for a better understanding of insole structures, thus facilitating the prescription of suitable insoles for diabetic patients to offer optimal foot protection from ulcers.

Declaration of competing interest

The authors declare that they have no known competing interests.

Acknowledgement

This research is funded by the Laboratory for Artificial Intelligence in Design (Project: RP1-2), Innovation and Technology Fund, Hong Kong.

References

1. J P Pollard, L P Le Quesne, and J W Tappin. Forces under the foot. Journal of Biomedical Engineering 5 (1983): 37-40.
2. J J van Netten, P A Lazzarini, D G Armstrong, et al. Diabetic Foot Australia guideline on footwear for people with diabetes. Journal of Foot and Ankle Research 11 (2018).
3. K B Bhagavathula, C S Meredith, S Ouellet, et al. Density, strain rate and strain effects on mechanical property evolution in polymeric foams. International Journal of Impact Engineering 161 (2022).
4. D Hernández-Lara, R G Rodríguez-Cañizo, E A Merchán-Cruz, et al. Optimal design of a foot prosthesis insole with composite materials applying metaheuristic algorithms. Results in Engineering 13 (2022).
5. M Curryer and E D Lemaire. Effectiveness of various materials in reducing plantar shear forces: A pilot study. Journal of the American Podiatric Medical Association 90 (2000): 346-353.
6. W T Lo, D P Wong, K L Yick, et al. Effects of custom-made textile insoles on plantar pressure distribution and lower limb EMG activity during turning. Journal of Foot and Ankle Research 9 (2016).
7. F Nilsen, M Molund, E M Lium, et al. Material Selection for Diabetic Custom Insoles: A Systematic Review of Insole Materials and Their Properties. Journal of Prosthetics and Orthotics 34 (2022): 131-143.
8. D Werner, J Maier, N Kaube, et al. Tailoring of Hierarchical Porous Freeze Foam Structures. Materials 15 (2022).
9. A N Natali, E L Carniel, A Frigo, et al. Experimental investigation of the structural behavior of equine urethra. Computer Methods and Programs in Biomedicine 141(2017): 35-41.
10. R Montuori, E Nastri, V Piluso, et al. Performance-based rules for the simplified assessment of steel CBFs. Journal of Constructional Steel Research 191 (2022).
11. R Ullah, M Vafaei, S C Alih, et al. A review of buckling-restrained braced frames for seismic protection of structure. Physics and Chemistry of the Earth 128 (2022).
12. R Sabelli, S Mahin, and C Chang. Seismic demands on steel braced frame buildings with buckling-restrained braces. Engineering Structures 25 (2003): 655-666.
13. D A Skolnik and J W Wallace. Critical assessment of interstory drift measurements. Journal of Structural Engineering 136 (2010): 1574-1584.
14. L Wang, D Jones, G J Champman, et al. An Inductive Force Sensor for In-Shoe Plantar Normal and Shear Load Measurement. IEEE Sensors Journal 20 (2020): 13318-13331.
15. T Y Yang, H Sheikh, and L Tobber. Influence of the brace configurations on the seismic performance of steel concentrically braced frames. Frontiers in Built Environment 5 (2019).
16. P E Chatzistergos and N Chockalingam. An in vivo model for overloading-induced soft tissue injury. Scientific Reports 12 (2022).
17. M S H Leung, K L Yick, Y Sun, et al. 3D printed auxetic heel pads for patients with diabetic mellitus. Computers in Biology and Medicine 146 (2022).
18. A A Chagas Paz, M A de Souza, P W Brock, et al. Finite element analysis to predict temperature distribution in the human neck with abnormal thyroid: A proof of concept. Computer Methods and Programs in Biomedicine 227 (2022).
19. H Shaulian, A Gefen, D Solomonow-Avnon, et al. Finite element-based method for determining an optimal

Leung MS., et al., Fortune J Rheumatol 2024
DOI:10.26502/fjr.26880042

offloading design for treating and preventing heel ulcers. Computers in Biology and Medicine 131 (2021).

20. J T M Cheung and M Zhang. A 3-dimensional finite element model of the human foot and ankle for insole design. Archives of Physical Medicine and Rehabilitation 86 (2005): 353-358.

21. A Gefen, M Megido-Ravid, Y Itzchak, et al. Biomechanical analysis of the three-dimensional foot structure during gait: A basic tool for clinical applications. Journal of Biomechanical Engineering 122 (2000): 630-639.

22. J T M Cheung, M Zhang, A K L Leung, et al. Three-dimensional finite element analysis of the foot during standing - A material sensitivity study. Journal of Biomechanics 38 (2005): 1045-1054.

23. R W Ogden, Large deformation isotropic elasticity - on the correlation of theory and experiment for incompressible rubberlike solids. Rubber Chemistry and Technology 46 (1973): 398-416.

24. T Yamaguchi, K Shibata, H Wada, et al. Effect of foot–floor friction on the external moment about the body center of mass during shuffling gait: a pilot study Scientific Reports 11 (2021).